

Supporting Information

Dehydration of Niclosamide Monohydrate Polymorphs: Different Mechanistic Pathways to the Same Product

Jen E. Mann, Renee Gao, and Jennifer A. Swift*

Georgetown University, Department of Chemistry, Washington, DC 20057-1227

Table of Contents	Page
Figure S1. Optical images of (left) H _A and (right) H _B taken at the same magnification. Both monohydrates exhibit a needle-like morphology. H _A crystallizes as fine needles, while H _B crystallizes as clusters of thick needles. Scale bars = 500 μm.	3
Figure S2. DSC curves of heat flow vs. temperature for H _A samples that were (A) ground with a mortar and pestle and (B) unground. DSC samples were heated at 5 °C/min to 250 °C in aluminum pans with unsealed lids.	3
Figure S3. Change in peak intensity for (130), (042), (113), and (112) diffraction lines with temperature. From 22 to 75 °C, the peaks decrease by 5.0%, 6.1%, 6.4% and 18.5%, respectively.	4
Figure S4. Change in cell volume and beta angle of the H _A (and/or H*) lattice from 22 to 150 °C determined from Pawley refinement of sPXRD data.	4
Figure S5. Contour plots of two additional H _A dehydration experiments performed under similar heating conditions. (Left) H _A was heated to 150 °C and held isothermally for 30 minutes. H* remained stable. (Right) The H* to F1 conversion occurred below 150 °C.	5
Table S1. Regression parameters associated with different solid state reaction models for isothermal TGA data (40, 45, and 50 °C) for H _A (ground). Reaction models with the highest statistical fit are indicated, with R ² > 0.99 in red.	6
Figure S6. (A) Summary of E _a determination from three runner-up model-based kinetic analyses of isothermal TGA data on H _A collected at 40, 45 and 50°C. (B) Arrhenius plot. All four models with the highest R ² coefficients yielded similar E _a values. (C) E _a vs. alpha calculated from the model-free Friedman analysis method. (D) E _a vs. alpha calculated using the standard model-free method.	7
Figure S7. TGA of ground H _B in open pans heated at 5 °C/min.	7

Figure S8. Change in cell volume and beta angle of the H_B lattice from 25 to 120 °C determined from Pawley refinement of sPXRD data. **8**

Figure S9. Fraction dehydrated (α) vs. time plots for H_B based on triplicate isothermal TGA data collected at 40, 45 and 50 °C. Inset plot is an expanded view of the data from 0 – 100 min. All samples were ground and heated at 5 °C/min. **8**

Table S2. Regression parameters associated with different solid state reaction models for isothermal TGA data (40, 45, and 50 °C) for H_B (ground). Reaction models with the highest statistical fit are indicated, with $R^2 > 0.99$ in red. Ones with $R^2 > 0.999$ are in bold. **9**

Figure S10. (A) Summary of E_a determination from two runner-up model-based kinetic analyses of isothermal TGA data on H_B collected at 40, 45 and 50°C. (B) Arrhenius plot. All models with $R^2 > 0.99$ coefficients yielded similar E_a values. (C) E_a vs. alpha calculated from the model-free Friedman analysis method. (D) E_a vs. alpha calculated using the standard model-free method. **10**

Figure S11. sPXRD of three different ground batches of H_B compared against the PXRD patterns of HB and F1 simulated from the single crystal structures. (left) A zoomed view of the region where high intensity peaks would be expected if F1 was present in the samples. **11**

Figure S12. Hot-stage microscopy optical images of H_B ramped at 5 °C/min from room temperature to 150 °C. At approximately 95 °C dark spots begin to appear across the surface until 140 °C whereupon optical changes can no longer be observed. Scale bar = 100 μ m. **11**

Figure S13. (left) Calculated BFDH morphology and (right) top ten slip planes calculated using the CSD-Particle module in the Cambridge Structural Database. None of the calculated slip planes correspond to the natural faces. **12**

Figure S14. Schematic of packing in H_B and F1. Each NCL molecule is colored so that the nitrophenyl ring is orange and the phenol ring is light blue. Water molecules in H_B are dark blue. **12**

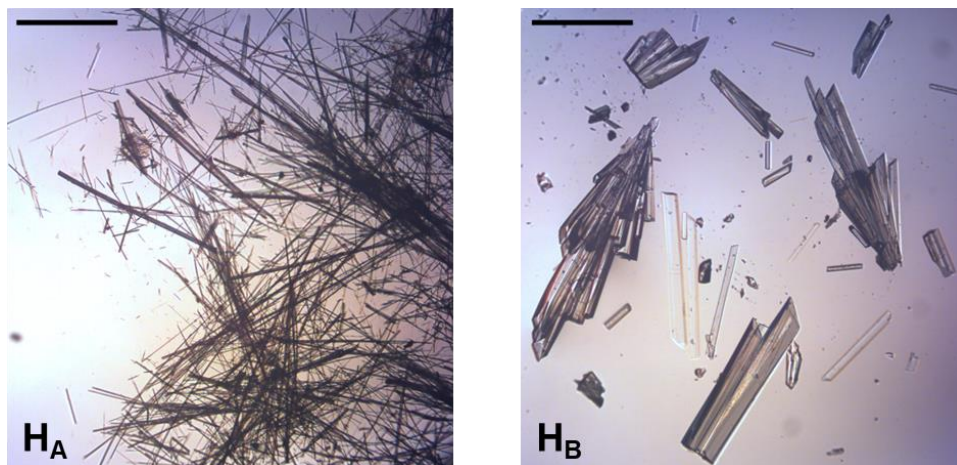


Figure S1. Optical images of (left) H_A and (right) H_B taken at the same magnification. Both monohydrates exhibit a needle-like morphology. H_A crystallizes as fine needles, while H_B crystallizes as clusters of thick needles. Scale bars = 500 μ m.

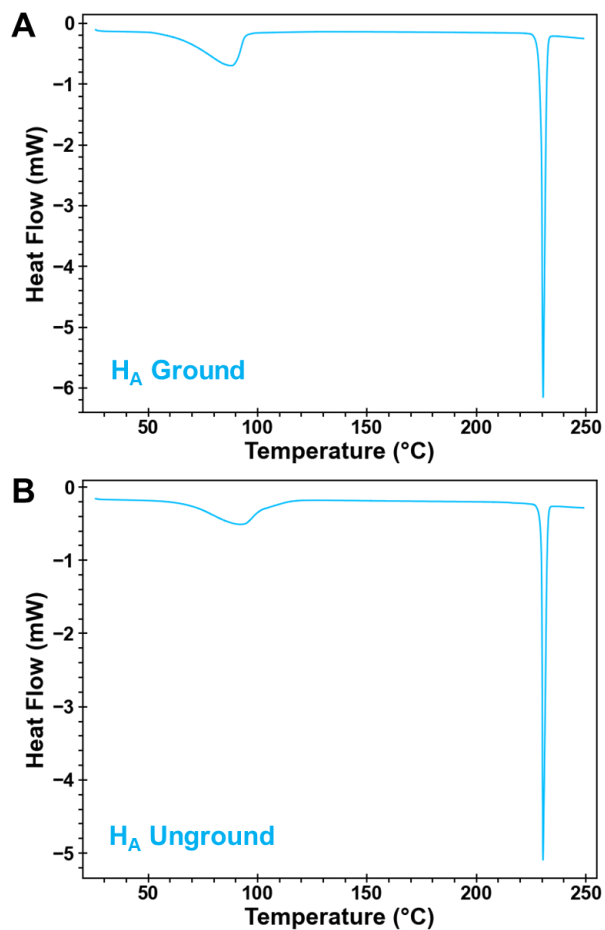


Figure S2. DSC curves of heat flow vs. temperature for H_A samples that were (A) ground with a mortar and pestle and (B) unground. DSC samples were heated at 5 $^{\circ}$ C/min to 250 $^{\circ}$ C in aluminum pans with unsealed lids.

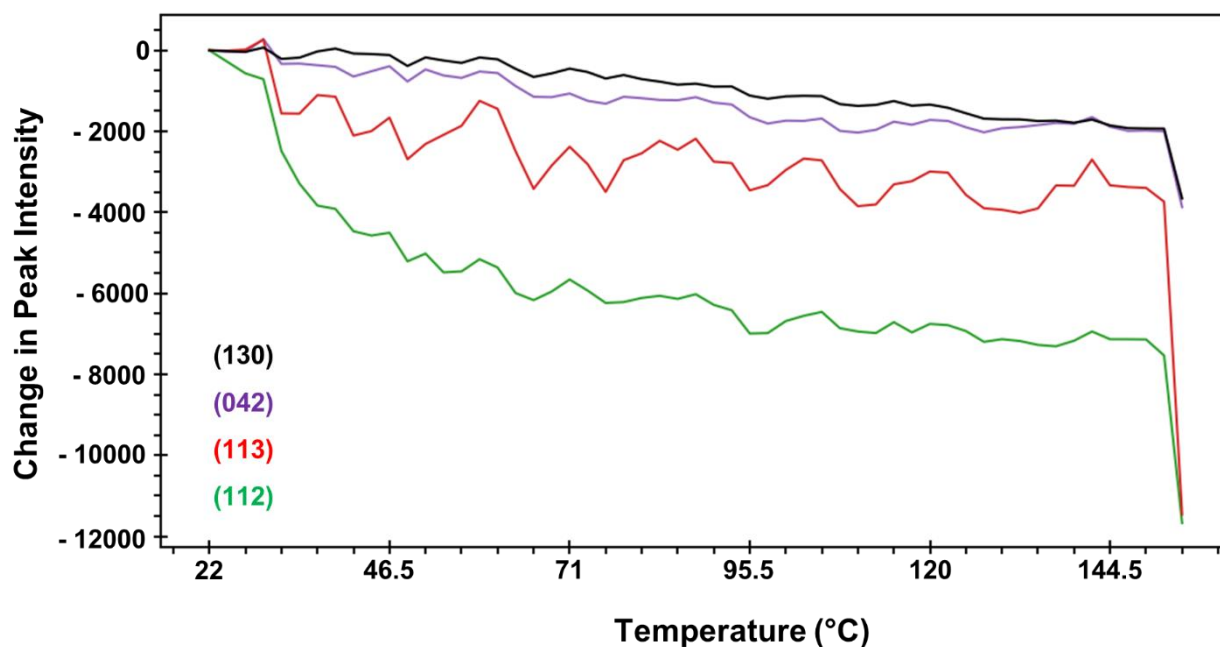


Figure S3. Change in peak intensity for (130), (042), (113), and (112) diffraction lines with temperature. From 22 to 75 °C, the peaks decrease by 5.0%, 6.1%, 6.4% and 18.5%, respectively.

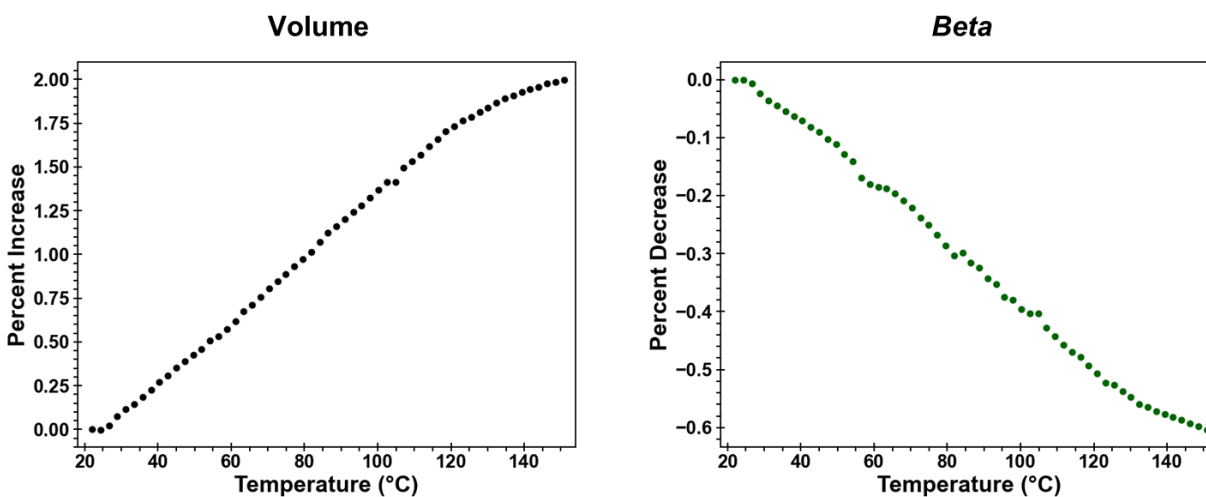


Figure S4. Change in cell volume and beta angle of the H_A (and/or H^*) lattice from 22 to 150 °C determined from Pawley refinement of sPXRD data.

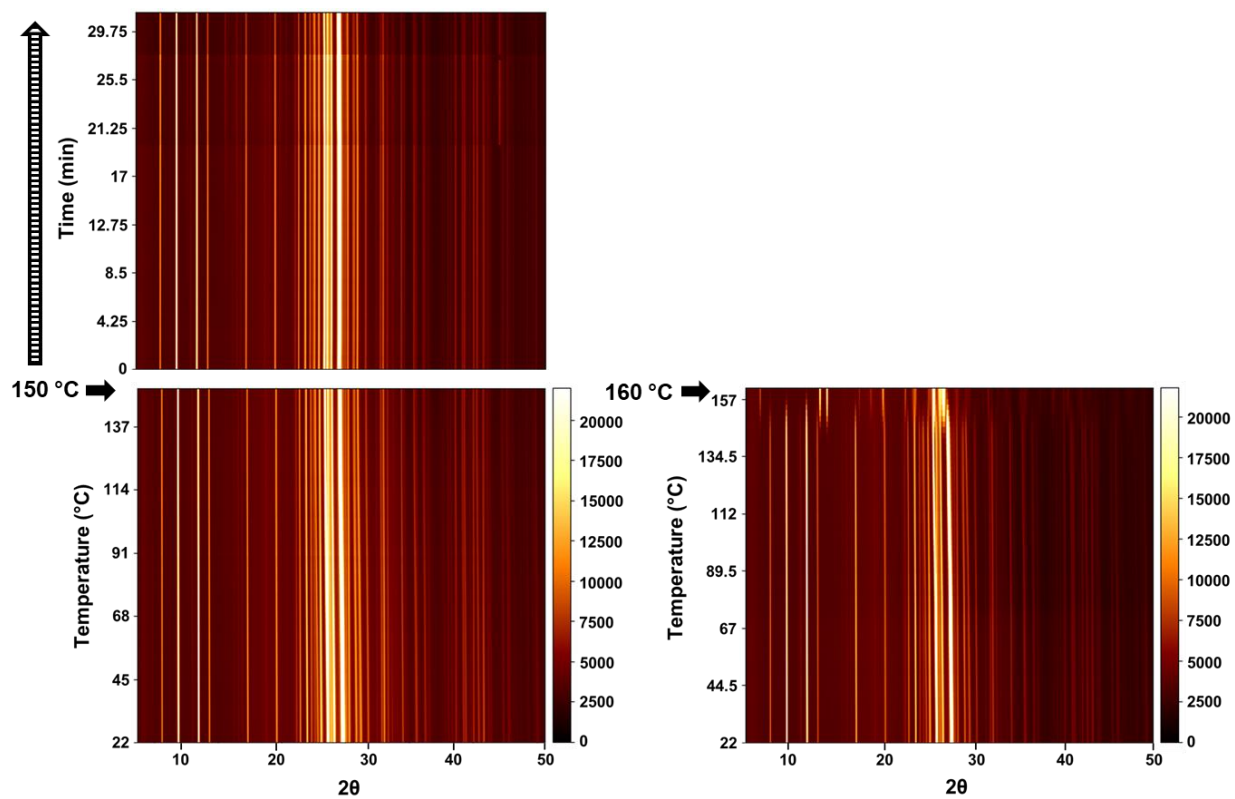


Figure S5. Contour plots of two additional H_A dehydration experiments performed under similar heating conditions. (Left) H_A was heated to 150 °C and held isothermally for 30 minutes. H^* remained stable. (Right) The H^* to F1 conversion occurred below 150 °C.

Table S1. Regression parameters associated with different solid state reaction models for isothermal TGA data (40, 45, and 50 °C) for H_A (ground). Reaction models with the highest statistical fit are indicated, with R² > 0.99 in red.

	40 °C	45 °C	50 °C
Nucleation Models			
1D growth of nuclei (Avrami-Erofeyev Eq, n = 2) (A2)	0.99525	0.99487	0.99584
2D growth of nuclei (Avrami-Erofeyev Eq, n = 3) (A3)	0.98554	0.98414	0.98482
3D growth of nuclei (Avrami-Erofeyev Eq, n = 4) (A4)	0.97760	0.97573	0.97624
Random nucleation (Prout-Tompkins Eq) (B1)	0.98836	0.98719	0.98794
Power law (n = 1/2) (P2)	0.93286	0.92775	0.92840
Power law (n = 1/3) (P3)	0.91164	0.90591	0.90649
Power law (n = 1/4) (P4)	0.89966	0.89360	0.89415
Geometrical Contraction Models			
2D phase boundary (Contracting area) (R2)	0.99701	0.99687	0.99800
3D phase boundary (Contracting volume) (R3)	0.99688	0.99788	0.99906
Diffusion Models			
1D diffusion (D1)	0.99194	0.99307	0.99419
2D diffusion (D2)	0.97794	0.98209	0.98305
3D diffusion (Jander Eq) (D3)	0.93565	0.94428	0.94470
3D Diffusion (Ginstling-Brounshtein Eq) (D4)	0.96644	0.97206	0.97287
Reaction Order Models			
Zero-order (R1)	0.97565	0.97243	0.97339
First-order (F1)	0.98393	0.98746	0.98865
Second-order (F2)	0.85251	0.86649	0.86627
Third-order (F3)	0.66572	0.69136	0.68855

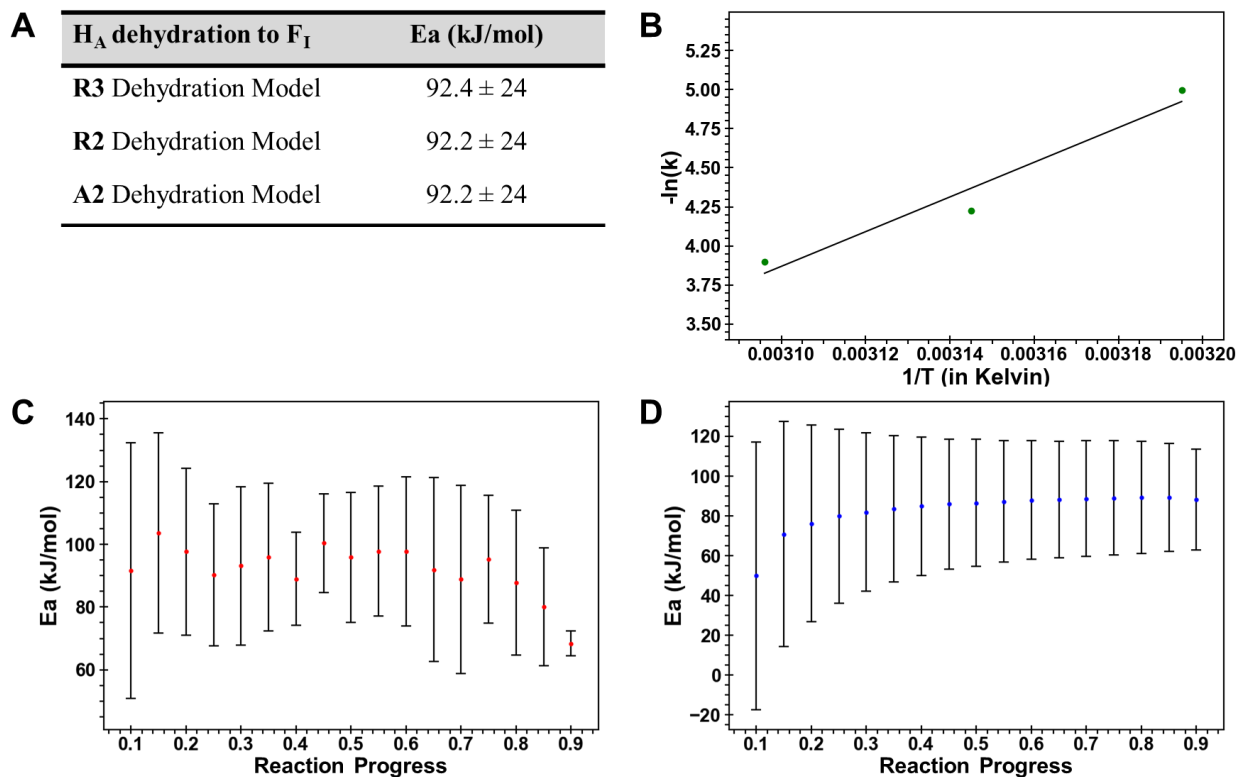


Figure S6. (A) Summary of E_a determination from three runner-up model-based kinetic analyses of isothermal TGA data on H_A collected at 40, 45 and 50°C. (B) Arrhenius plot. All four models with the highest R^2 coefficients yielded similar E_a values. (C) E_a vs. alpha calculated from the model-free Friedman analysis method. (D) E_a vs. alpha calculated using the standard model-free method.

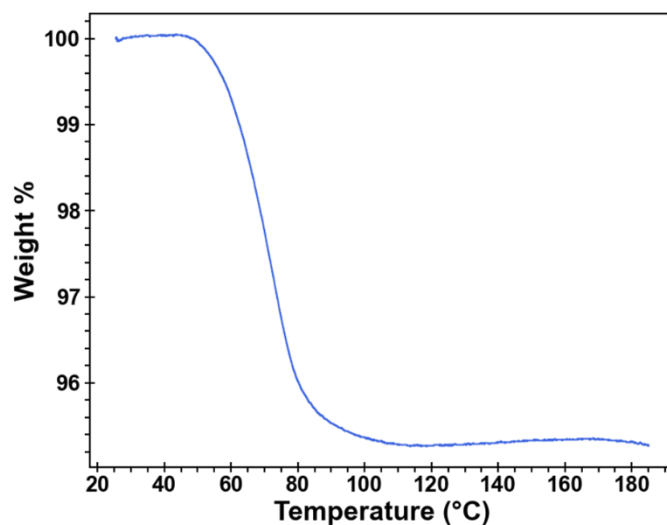


Figure S7. TGA of ground H_B in open pans heated at 5 °C/min.

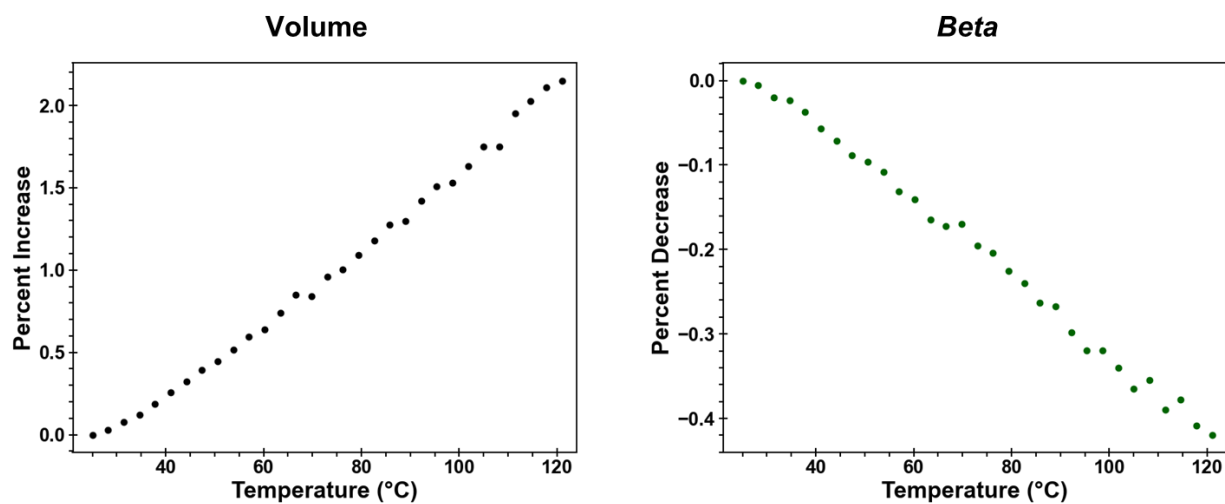


Figure S8. Change in cell volume and beta angle of the H_B lattice from 25 to 120 °C determined from Pawley refinement of sPXRD data.

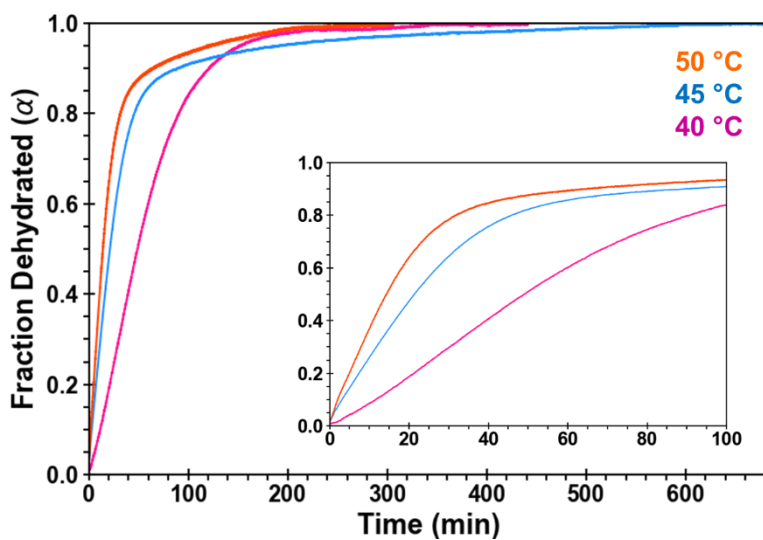


Figure S9. Fraction dehydrated (α) vs. time plots for H_B based on triplicate isothermal TGA data collected at 40, 45 and 50 °C. Inset plot is an expanded view of the data from 0 – 100 min. All samples were ground and heated at 5 °C/min.

Table S2. Regression parameters associated with different solid state reaction models for isothermal TGA data (40, 45, and 50 °C) for H_B (ground). Reaction models with the highest statistical fit are indicated, with R² > 0.99 in red. Ones with R² > 0.999 are in bold.

	40 °C	45 °C	50 °C
Nucleation Models			
1D growth of nuclei (Avrami-Erofeyev Eq, n = 2) (A2)	0.99551	0.98342	0.98556
2D growth of nuclei (Avrami-Erofeyev Eq, n = 3) (A3)	0.98544	0.96816	0.97131
3D growth of nuclei (Avrami-Erofeyev Eq, n = 4) (A4)	0.97800	0.95825	0.96199
Random nucleation (Prout-Tompkins Eq) (B1)	0.98756	0.97178	0.97473
Power law (n = 1/2) (P2)	0.95525	0.92620	0.93163
Power law (n = 1/3) (P3)	0.93763	0.90561	0.91217
Power law (n = 1/4) (P4)	0.92753	0.89409	0.90125
Geometrical Contraction Models			
2D phase boundary (Contracting area) (R2)	0.99919	0.99180	0.99289
3D phase boundary (Contracting volume) (R3)	0.99909	0.99573	0.99642
Diffusion Models			
1D diffusion (D1)	0.98996	0.99368	0.99312
2D diffusion (D2)	0.97509	0.98915	0.98804
3D diffusion (Jander Eq) (D3)	0.94598	0.97205	0.97073
3D Diffusion (Ginstling-Brounshtein Eq) (D4)	0.96649	0.98471	0.98349
Reaction Order Models			
Zero-order (R1)	0.98851	0.96955	0.97224
First-order (F1)	0.99300	0.99786	0.99794
Second-order (F2)	0.92988	0.95964	0.95921
Third-order (F3)	0.82239	0.87390	0.87413

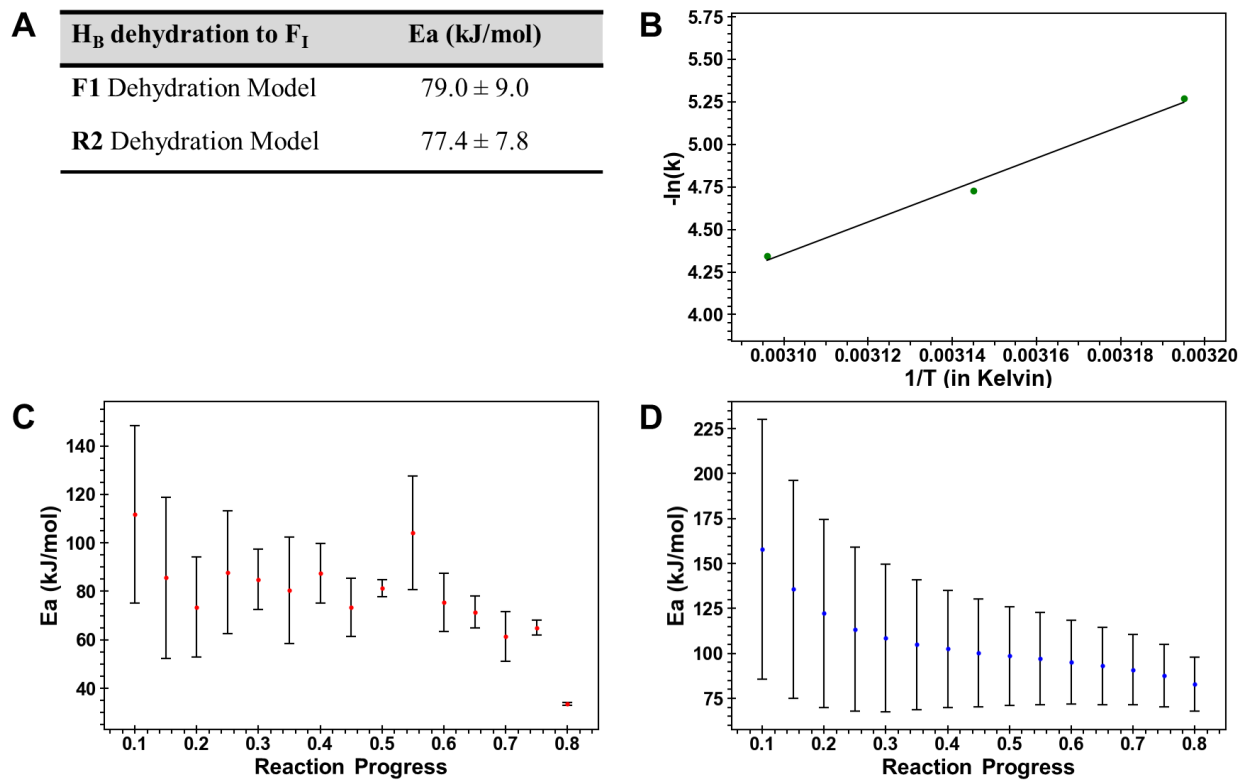


Figure S10. (A) Summary of E_a determination from two runner-up model-based kinetic analyses of isothermal TGA data on H_B collected at 40, 45 and 50°C. (B) Arrhenius plot. All models with $R^2 > 0.99$ coefficients yielded similar E_a values. (C) E_a vs. α calculated from the model-free Friedman analysis method. (D) E_a vs. α calculated using the standard model-free method.

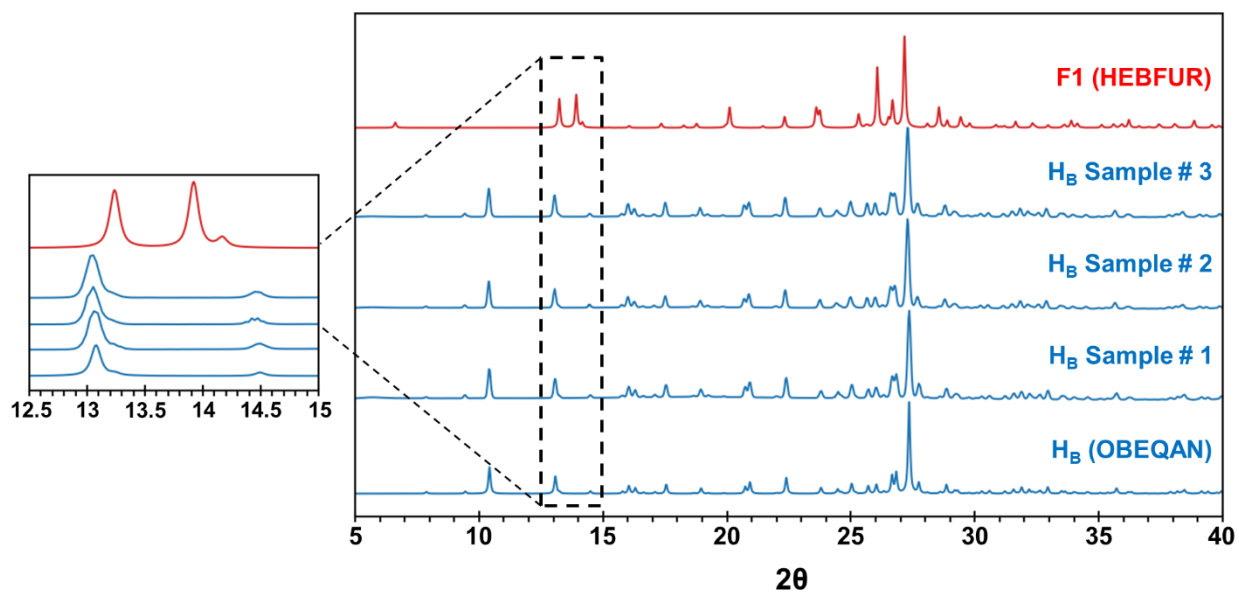


Figure S11. sPXRD of three different ground batches of H_B compared against the PXRD patterns of HB and F1 simulated from the single crystal structures. (left) A zoomed view of the region where high intensity peaks would be expected if F1 was present in the samples.

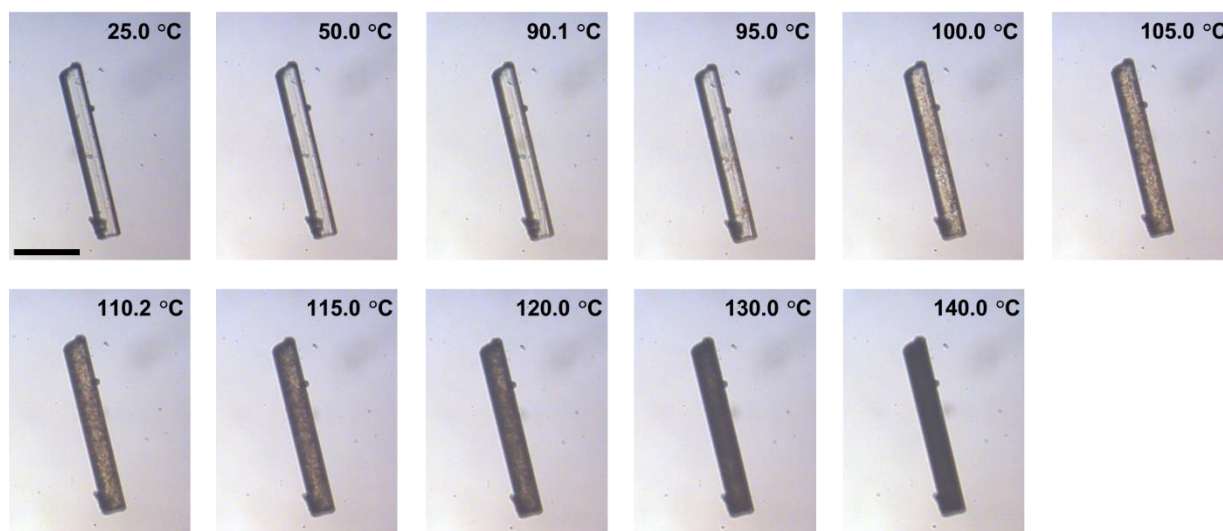


Figure S12. Hot-stage microscopy optical images of H_B ramped at 5 °C/min from room temperature to 150 °C. At approximately 95 °C dark spots begin to appear across the surface until 140 °C whereupon optical changes can no longer be observed. Scale bar = 100 μm.

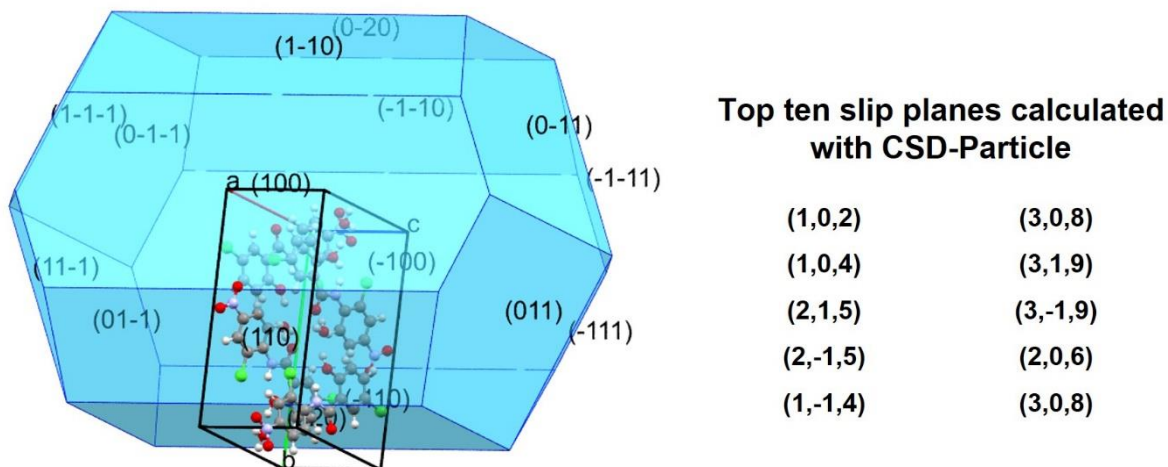


Figure S13. (left) Calculated BFDH morphology and (right) top ten slip planes calculated using the CSD-Particle module in the Cambridge Structural Database. None of the calculated slip planes correspond to the natural faces.

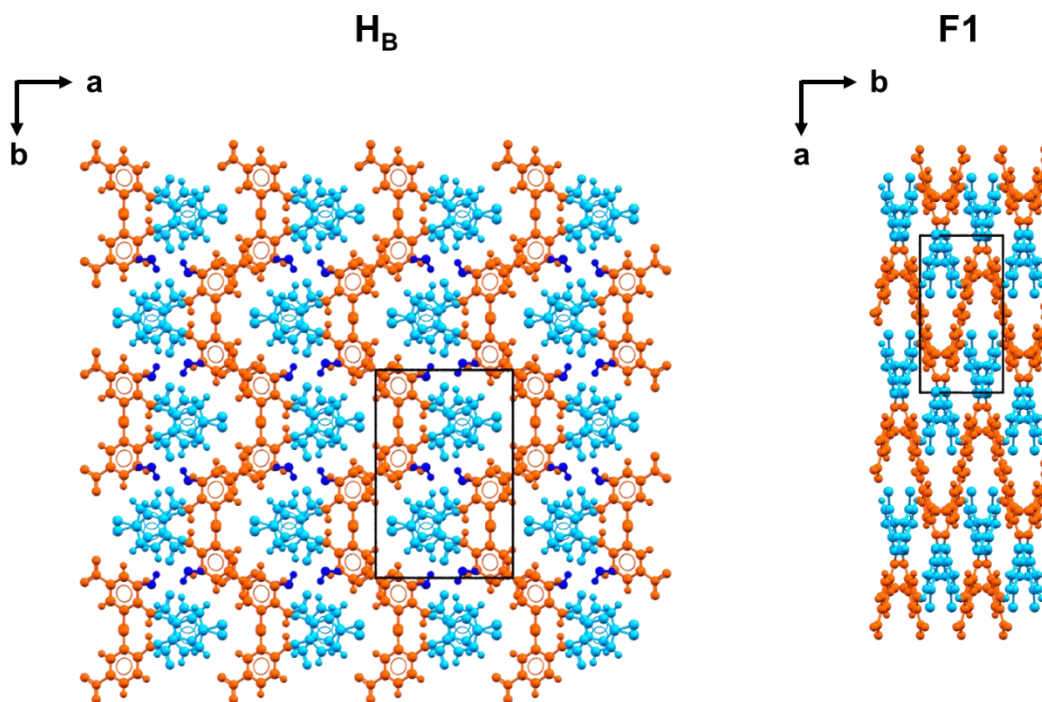


Figure S14. Schematic of packing in H_B and F1. Each NCL molecule is colored so that the nitrophenyl ring is orange and the phenol ring is light blue. Water molecules in H_B are dark blue.